

# Longitudinal-Torsional and Two Plane Transverse Vibrations of a Composite Timoshenko Rotor

M. Irani Rahagi\*, A. Mohebbi, H. Afshari

*Department of Solid Mechanics, Faculty of Mechanical Engineering, University of Kashan, Kashan, Iran*

Received 22 March 2016; accepted 18 May 2016

## ABSTRACT

In this paper, two kinds of vibrations are considered for a composite Timoshenko rotor: longitudinal-torsional vibration and two plane transverse one. The kinetic and potential energies and virtual work due to the gyroscopic effects are calculated and the set of six governing equations and boundary conditions are derived using Hamilton principle. Differential quadrature method (DQM) is used as a strong numerical method and natural frequencies and mode shapes are derived. Effects of the rotating speed and the lamination angle on the natural frequencies are studied for various boundary conditions; meanwhile, critical speeds of the rotor are determined. Two kinds of critical speeds are considered for the rotor: the resonance speed, which happens as rotor rotates near one of the natural frequencies, and the instability speed, which occurs as value of the first natural frequency decreases to zero and rotor becomes instable.

© 2016 IAU, Arak Branch. All rights reserved.

**Keywords :** Longitudinal-torsional vibration; Transverse vibration; Composite rotor; DQM.

## 1 INTRODUCTION

SINCE composite materials have the potential of the innovative and cost effective manufacturing technology, they have attracted a lot of attention for thick or thin structures. A number of different elements of composite structures such as aircraft wings, helicopter rotor blades, robots arms, bridges and structural elements in civil engineering constructions can be idealized as thin- or thick-walled beams, which can be studied by considering simpler governing equations. Zu et al. [1] have investigated the free vibration behavior of a spinning metallic beam, where the classical theory of differential equations which couple flexural motions in both principal planes, but ignores torsional deformation is used, with general boundary conditions. In another study, Zu et al. [2] considered natural frequencies and normal modes for externally damped spinning Timoshenko beam with general boundary conditions. Reis et al. [3] published analytical investigations on thin-walled layered composite cylindrical tubes, concluding that bending-stretching coupling and shear-normal coupling effects will alter the frequency values. A research was conducted by Gupta and Singh [4] on the effects of shear-normal coupling on rotor natural frequencies and modal damping. Amongst all the investigators, it seems that Bert [5] is the first one who presented a simple method for critical speed analysis of composite shafts by taking coupled bending-torsion composite beam theory into consideration. Before long, Kim and Bert [6] used a more accurate shell theory for composite shaft and made a direct comparison with the beam theory. In another attempt, Banerjee and Su [7] developed the dynamic stiffness matrix for spinning composite beam by including bending-torsion coupling effects and then analyzed free vibration characteristics. Chang et al. [8] published the vibration behaviors of the rotating composite shafts. In the model, the

\*Corresponding author. Tel.: +98 31 55912420; Fax: +98 31 55559930.  
E-mail address: [irani@kashanu.ac.ir](mailto:irani@kashanu.ac.ir) (M. Irani Rahagi).

transverse shear deformation, rotary inertia, and gyroscopic effects, as well as the coupling effects due to the lamination of composite layers have been incorporated.

In this paper, longitudinal-torsional and two plane transverse vibrations of a composite Timoshenko rotor are investigated. Shear deformation, rotating inertia and gyroscopic effect are considered. Differential quadrature method is employed and natural frequencies and mode shapes are derived numerically. Effects of the rotating speed and the lamination angle on the natural frequencies are studied for various boundary conditions; meanwhile, critical speeds of the rotor are determined.

## 2 THE GOVERNING EQUATION AND BOUNDARY CONDITION

As depicted in Fig. 1, a composite rotor rotating at a constant angular velocity is considered. The following displacement field is assumed by choosing the coordinate axis  $x$  to coincide with the shaft axis [9]:

$$\begin{aligned} U(x, y, z, t) &= U_0(x, t) + z\beta_y(x, t) - y\beta_z(x, t) \\ V(x, y, z, t) &= V_0(x, t) - z\phi(x, t) \\ W(x, y, z, t) &= W_0(x, t) + y\phi(x, t) \end{aligned} \quad (1)$$

where  $U$ ,  $V$  and  $W$  are displacements of any point on the cross-section of the shaft in the  $x$ ,  $y$  and  $z$  directions, respectively;  $U_0$ ,  $V_0$  and  $W_0$  are value of the  $U$ ,  $V$  and  $W$  on the shaft's axis, while  $\beta_x$  and  $\beta_y$  are rotation angles of the cross-section, about the  $y$  and  $z$  axes, respectively and  $\phi$  is the angular rotation of the cross-section due to the torsion deformation of the shaft.

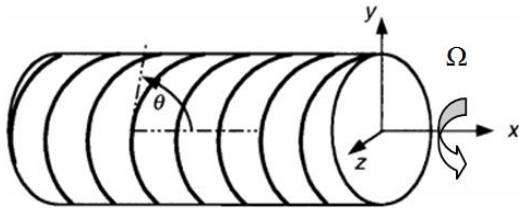


**Fig.1**  
Composite rotor.

The velocity of each point on the shaft can be stated as:

$$\vec{v} = \dot{\vec{r}} + \vec{\Omega} \times \vec{r} \quad (2)$$

In which

$$\vec{\Omega} = \Omega \vec{i} \quad (3)$$

Substituting Eqs. (1) and (3) for Eq. (2), the velocity of each point on the shaft can be derived as:

$$\vec{v} = \left( \frac{\partial U_0}{\partial t} + z \frac{\partial \beta_y}{\partial t} - y \frac{\partial \beta_z}{\partial t} \right) \vec{i} + \left( \frac{\partial V_0}{\partial t} - z \frac{\partial \phi}{\partial t} - \Omega W_0 - y \Omega \phi \right) \vec{j} + \left( \frac{\partial W_0}{\partial t} + y \frac{\partial \phi}{\partial t} + \Omega V_0 - z \Omega \phi \right) \vec{k} \quad (4)$$

Kinetic energy of the shaft can be stated as:

$$E_k = \frac{1}{2} \int_0^L \int_A \rho \vec{v} \cdot \vec{v} dA dx \quad (5)$$

where  $\rho$  is density of the shaft. Using Eqs. (4) and (5), kinetic energy can be stated as:

$$E_k = \frac{1}{2} I_m \int_0^L \left\{ \left( \frac{\partial U_0}{\partial t} \right)^2 + \left( \frac{\partial V_0}{\partial t} \right)^2 + \left( \frac{\partial W_0}{\partial t} \right)^2 + \Omega^2 (W_0^2 + V_0^2) + 2\Omega \left( V_0 \frac{\partial W_0}{\partial t} - W_0 \frac{\partial V_0}{\partial t} \right) \right\} dx$$

$$+ \frac{1}{2} I_p \int_0^L \left[ \left( \frac{\partial \phi}{\partial t} \right)^2 + \Omega^2 \phi^2 \right] dx + \frac{1}{2} I_d \int_0^L \left[ \left( \frac{\partial \beta_y}{\partial t} \right)^2 + \left( \frac{\partial \beta_z}{\partial t} \right)^2 \right] dx$$
(6)

In which mass, transverse and polar mass moment of inertias of the rotor are defined respectively as:

$$I_m = \int_A \rho dA \quad I_d = \int_A \rho y^2 dA = \int_A \rho z^2 dA \quad I_p = \int_A \rho (y^2 + z^2) dA = 2I_d$$
(7)

For a composite rotor with k layers, these parameters can be calculated using following relations:

$$I_m = \pi \sum_{n=1}^k \rho_n (R_n^2 - R_{n-1}^2) \quad I_d = \frac{\pi}{4} \sum_{n=1}^k \rho_n (R_n^4 - R_{n-1}^4) \quad I_p = \frac{\pi}{2} \sum_{n=1}^k \rho_n (R_n^4 - R_{n-1}^4) = 2I_d$$
(8)

where  $\rho_n, R_{n-1}$  and  $R_n$  are density, inner and outer radius of the  $n^{th}$  layer, respectively.

Applying the relation between stress and strain in the composite materials and strain-displacement relations in the cylindrical coordinate, the potential energy of the rotor can be derived as [9]:

$$E_u = \frac{1}{2} A_{11} \int_0^L \left( \frac{\partial U_0}{\partial x} \right)^2 dx + \frac{1}{2} B_{11} \int_0^L \left[ \left( \frac{\partial \beta_y}{\partial x} \right)^2 + \left( \frac{\partial \beta_z}{\partial x} \right)^2 \right] dx + \frac{1}{2} k B_{66} \int_0^L \left( \frac{\partial \phi}{\partial x} \right)^2 dx +$$

$$\frac{1}{2} k A_{16} \int_0^L \left[ 2 \frac{\partial \phi}{\partial x} \frac{\partial U_0}{\partial x} + \beta_z \frac{\partial \beta_y}{\partial x} - \beta_y \frac{\partial \beta_z}{\partial x} - \frac{\partial V_0}{\partial x} \frac{\partial \beta_y}{\partial x} - \frac{\partial W_0}{\partial x} \frac{\partial \beta_z}{\partial x} \right] dx +$$

$$\frac{1}{2} k (A_{55} + A_{66}) \int_0^L \left[ \left( \frac{\partial V_0}{\partial x} \right)^2 + \left( \frac{\partial W_0}{\partial x} \right)^2 + \beta_y^2 + \beta_z^2 + 2\beta_y \frac{\partial W_0}{\partial x} - 2\beta_z \frac{\partial V_0}{\partial x} \right] dx$$
(9)

In which the following axial, polar and transverse flexural rigidities are defined:

$$A_{11} = \pi \sum_{n=1}^k C'_{11n} (R_n^2 - R_{n-1}^2) \quad A_{16} = \frac{2\pi}{3} \sum_{n=1}^k C'_{16n} (R_n^3 - R_{n-1}^3)$$

$$A_{55} = \frac{\pi}{2} \sum_{n=1}^k C'_{55n} (R_n^2 - R_{n-1}^2) \quad B_{11} = \frac{\pi}{4} \sum_{n=1}^k C'_{11n} (R_n^4 - R_{n-1}^4)$$

$$A_{66} = \frac{\pi}{2} \sum_{n=1}^k C'_{66n} (R_n^2 - R_{n-1}^2) \quad B_{66} = \frac{\pi}{2} \sum_{n=1}^k C'_{66n} (R_n^4 - R_{n-1}^4)$$
(10)

and  $C'_{in}$  are the effective elastic constants of the  $n^{th}$  layer which are introduced in Appendix A.

Also, the virtual work due to the gyroscopic moments can be considered as [10]:

$$\delta W = I_p \Omega \int_0^L \left( \frac{\partial \beta_y}{\partial t} \delta \beta_z - \frac{\partial \beta_z}{\partial t} \delta \beta_y \right) dx$$
(11)

Now, using Hamilton principle as:

$$\delta \int_{t_1}^{t_2} (E_k + W - E_u) dt = 0$$
(12)

The set of governing equations and boundary conditions can be derived as:

$$\begin{aligned}
\delta U_0 : A_{11} \frac{\partial^2 U_0}{\partial x^2} + kA_{16} \frac{\partial^2 \phi}{\partial x^2} - I_m \frac{\partial^2 U_0}{\partial t^2} &= 0 \\
\delta \phi : kA_{16} \frac{\partial^2 U_0}{\partial x^2} + kB_{66} \frac{\partial^2 \phi}{\partial x^2} + I_p \left( \Omega^2 \phi - \frac{\partial^2 \phi}{\partial t^2} \right) &= 0 \\
\delta V_0 : \frac{1}{2} kA_{16} \frac{\partial^2 \beta_y}{\partial x^2} + k (A_{55} + A_{66}) \left( \frac{\partial \beta_z}{\partial x} - \frac{\partial^2 V_0}{\partial x^2} \right) - I_m \left( \Omega^2 V_0 + 2\Omega \frac{\partial W_0}{\partial t} - \frac{\partial^2 V_0}{\partial t^2} \right) &= 0 \\
\delta W_0 : \frac{1}{2} kA_{16} \frac{\partial^2 \beta_z}{\partial x^2} - k (A_{55} + A_{66}) \left( \frac{\partial \beta_y}{\partial x} + \frac{\partial^2 W_0}{\partial x^2} \right) - I_m \left( \Omega^2 W_0 - 2\Omega \frac{\partial V_0}{\partial t} - \frac{\partial^2 W_0}{\partial t^2} \right) &= 0 \\
\delta \beta_y : \frac{1}{2} kA_{16} \frac{\partial^2 V_0}{\partial x^2} + k (A_{55} + A_{66}) \left( \beta_y + \frac{\partial W_0}{\partial x} \right) - kA_{16} \frac{\partial \beta_z}{\partial x} - B_{11} \frac{\partial^2 \beta_y}{\partial x^2} + I_p \Omega \frac{\partial \beta_z}{\partial t} + I_d \frac{\partial^2 \beta_y}{\partial t^2} &= 0 \\
\delta \beta_z : \frac{1}{2} kA_{16} \frac{\partial^2 W_0}{\partial x^2} + k (A_{55} + A_{66}) \left( \beta_z - \frac{\partial V_0}{\partial x} \right) + kA_{16} \frac{\partial \beta_y}{\partial x} - B_{11} \frac{\partial^2 \beta_z}{\partial x^2} - I_p \Omega \frac{\partial \beta_y}{\partial t} + I_d \frac{\partial^2 \beta_z}{\partial t^2} &= 0
\end{aligned} \tag{13a}$$

$$\begin{aligned}
\left( A_{11} \frac{\partial U_0}{\partial x} + kA_{16} \frac{\partial \phi}{\partial x} \right) \delta U_0 \Big|_{x=0}^{x=L} &= 0 \\
k \left( B_{66} \frac{\partial \phi}{\partial x} + A_{16} \frac{\partial U_0}{\partial x} \right) \delta \phi \Big|_{x=0}^{x=L} &= 0 \\
k \left[ \frac{1}{2} A_{16} \frac{\partial \beta_y}{\partial x} - (A_{55} + A_{66}) \left( \frac{\partial V_0}{\partial x} - \beta_z \right) \right] \delta V_0 \Big|_{x=0}^{x=L} &= 0 \\
k \left[ \frac{1}{2} A_{16} \frac{\partial \beta_z}{\partial x} - (A_{55} + A_{66}) \left( \frac{\partial W_0}{\partial x} + \beta_y \right) \right] \delta W_0 \Big|_{x=0}^{x=L} &= 0 \\
\left[ B_{11} \frac{\partial \beta_y}{\partial x} + \frac{1}{2} kA_{16} \left( \beta_z - \frac{\partial V_0}{\partial x} \right) \right] \delta \beta_y \Big|_{x=0}^{x=L} &= 0 \\
\left[ B_{11} \frac{\partial \beta_z}{\partial x} - \frac{1}{2} kA_{16} \left( \beta_y + \frac{\partial W_0}{\partial x} \right) \right] \delta \beta_z \Big|_{x=0}^{x=L} &= 0
\end{aligned} \tag{13b}$$

Applying method of separation of variables as:

$$\begin{aligned}
U_0(x, t) = Lu_0(x) e^{\omega t} \quad V_0(x, t) = Lv_0(x) e^{\omega t} \quad W_0(x, t) = Lw_0(x) e^{\omega t} \\
\beta_y(x, t) = \beta_y(x) e^{\omega t} \quad \beta_z(x, t) = \beta_z(x) e^{\omega t} \quad \phi(x, t) = \phi(x) e^{\omega t}
\end{aligned} \tag{14}$$

where  $\omega$  is natural frequency of vibration and also using following dimensionless parameters:

$$\begin{aligned}
\zeta = \frac{x}{L} \quad \gamma^2 = \frac{I_m L^2 \Omega^2}{A_{11}} \quad \lambda^2 = \frac{I_m L^2 \omega^2}{A_{11}} \quad \alpha_{16} = \frac{A_{16}}{A_{11} L} \quad \alpha_{55} = \frac{A_{55}}{A_{11}} \\
\alpha_{66} = \frac{A_{66}}{A_{11}} \quad \beta_{11} = \frac{B_{11}}{A_{11} L^2} \quad \beta_{66} = \frac{B_{66}}{A_{11} L^2} \quad \mu_d = \frac{I_d}{I_m L^2} \quad \mu_p = \frac{I_p}{I_m L^2} = 2\mu_d
\end{aligned} \tag{15}$$

In which  $L$  is the length of the rotor, dimensionless governing equation and boundary conditions can be rewritten as:

$$\begin{aligned}
 \frac{d^2 u_0}{d\zeta^2} + k \alpha_{16} \frac{d^2 \phi}{d\zeta^2} - \lambda^2 u_0 &= 0 \\
 k \alpha_{16} \frac{d^2 u_0}{d\zeta^2} + k \beta_{66} \frac{d^2 \phi}{d\zeta^2} + 2\mu_d \gamma^2 \phi - 2\mu_d \lambda^2 \phi &= 0 \\
 \frac{k \alpha_{16}}{2} \frac{d^2 \beta_y}{d\zeta^2} + k (\alpha_{55} + \alpha_{66}) \left( \frac{d \beta_z}{d\zeta} - \frac{d^2 v_0}{d\zeta^2} \right) - \gamma^2 v_0 - 2\gamma \lambda w_0 + \lambda^2 v_0 &= 0 \\
 \frac{k \alpha_{16}}{2} \frac{d^2 \beta_z}{d\zeta^2} - k (\alpha_{55} + \alpha_{66}) \left( \frac{d \beta_y}{d\zeta} + \frac{d^2 w_0}{d\zeta^2} \right) - \gamma^2 w_0 + 2\gamma \lambda v_0 + \lambda^2 w_0 &= 0 \\
 \frac{k \alpha_{16}}{2} \frac{d^2 v_0}{d\zeta^2} + k (\alpha_{55} + \alpha_{66}) \left( \beta_y + \frac{d w_0}{d\zeta} \right) - k \alpha_{16} \frac{d \beta_z}{d\zeta} - \beta_{11} \frac{d^2 \beta_y}{d\zeta^2} + 2\mu_d \gamma \lambda \beta_z + \mu_d \lambda^2 \beta_y &= 0 \\
 \frac{k \alpha_{16}}{2} \frac{d^2 w_0}{d\zeta^2} + k (\alpha_{55} + \alpha_{66}) \left( \beta_z - \frac{d v_0}{d\zeta} \right) + k \alpha_{16} \frac{d \beta_y}{d\zeta} - \beta_{11} \frac{d^2 \beta_z}{d\zeta^2} - 2\mu_d \gamma \lambda \beta_y + \mu_d \lambda^2 \beta_z &= 0
 \end{aligned}
 \tag{16a}$$

$$\begin{aligned}
 \frac{d u_0}{d\zeta} + k \alpha_{16} \frac{\partial \phi}{\partial \zeta} &= 0 \text{ or } u_0 = 0 \\
 \beta_{66} \frac{d \phi}{d\zeta} + \alpha_{16} \frac{d u_0}{d\zeta} &= 0 \text{ or } \phi = 0 \\
 \frac{\alpha_{16}}{2} \frac{d \beta_y}{d\zeta} - (\alpha_{55} + \alpha_{66}) \left( \frac{d v_0}{d\zeta} - \beta_z \right) &= 0 \text{ or } v_0 = 0 \\
 \frac{\alpha_{16}}{2} \frac{d \beta_z}{d\zeta} - (\alpha_{55} + \alpha_{66}) \left( \frac{d w_0}{d\zeta} + \beta_y \right) &= 0 \text{ or } w_0 = 0 \\
 \beta_{11} \frac{d \beta_y}{d\zeta} + \frac{k \alpha_{16}}{2} \left( \beta_z - \frac{d v_0}{d\zeta} \right) &= 0 \text{ or } \beta_y = 0 \\
 \beta_{11} \frac{d \beta_z}{d\zeta} - \frac{k \alpha_{16}}{2} \left( \beta_y + \frac{d w_0}{d\zeta} \right) &= 0 \text{ or } \beta_z = 0
 \end{aligned}
 \tag{16b}$$

As shown in Eq. (16), the coupled longitudinal-torsional vibrations and coupled two plane transverse vibration occur separately.

### 3 DIFFERENTIAL QUADRATURE METHOD (DQM)

The differential quadrature method is based on the idea that all derivatives of a function can be easily approximated by means of weighted linear sum of the function values at "N" pre-selected grid of points as:

$$\left. \frac{d^r f}{dx^r} \right|_{x=x_i} \approx \sum_{j=1}^N A_{ij}^{(r)} f_j
 \tag{17}$$

where  $A^{(r)}$  is the weighting coefficient associated with the  $r^{th}$  order derivative given by [11]

$$A_{ij}^{(1)} = \begin{cases} \frac{\prod_{\substack{m=1 \\ m \neq i, j}}^N (x_i - x_m)}{\prod_{\substack{m=1 \\ m \neq j}}^N (x_j - x_m)} & i, j = 1, 2, 3, \dots, N; i \neq j \\ \sum_{\substack{m=1 \\ m \neq i}}^N (x_i - x_m)^{-1} & i = j = 1, 2, 3, \dots, N \end{cases} \quad (18)$$

$$A_{ij}^{(r)} = A_{ij}^{(1)} A_{ij}^{(r-1)} \quad 2 \leq r \leq N - 1$$

In this paper, for simplifying, following notations are considered:

$$A = A^{(1)} \quad B = A^{(2)}. \quad (19)$$

Distribution of the grid points is an important aspect in convergence of the solution. A well-accepted set of the grid points is the Gauss–Lobatto–Chebyshev points given for interval  $[0, 1]$  as:

$$\bar{x}_i = \frac{1}{2} \left\{ 1 - \cos \left[ \frac{(i-1)\pi}{(N-1)} \right] \right\} \quad i = 1, 2, 3, \dots, N. \quad (20)$$

## 4 DQM SOLUTION

### 4.1 Longitudinal-torsional vibration

Using Eq. (17), the set of governing equation for longitudinal-torsional vibration can be written as:

$$[K_{lt}] \{p\} = \lambda^2 [M_{lt}] \{p\} \quad (21)$$

where

$$[K_{lt}] = \begin{bmatrix} [B] & k \alpha_{16} [B] \\ k \alpha_{16} [B] & k \beta_{66} [B] + 2\mu_d \gamma^2 I \end{bmatrix} \quad [M_{lt}] = \begin{bmatrix} I & 0 \\ 0 & 2\mu_d \end{bmatrix} \quad \{p\} = \begin{Bmatrix} \{u_0\} \\ \{\phi\} \end{Bmatrix} \quad (22)$$

and boundary conditions can be modeled as:

$$[T_{lt}] \{p\} = \{0\} \quad (23)$$

where matrix  $[T_{lt}]$  is presented in Appendix B for various boundary conditions.

### 4.2 Transverse vibration

Using Eq. (17), the set of governing equation for transverse vibration can be written as:

$$([K_t] + \lambda [C_t] + \lambda^2 [M_t]) \{q\} = \{0\} \quad (24)$$

where

$$\begin{aligned}
 [K_t] &= \begin{bmatrix} -k(\alpha_{55} + \alpha_{66})[B] - \gamma^2 I & [0] & 0.5k\alpha_{16}[B] & k(\alpha_{55} + \alpha_{66})[A] \\ [0] & -k(\alpha_{55} + \alpha_{66})[B] - \gamma^2 I & -k(\alpha_{55} + \alpha_{66})[A] & 0.5k\alpha_{16}[B] \\ 0.5k\alpha_{16}[B] & k(\alpha_{55} + \alpha_{66})[A] & k(\alpha_{55} + \alpha_{66})I - \beta_{11}[B] & -k\alpha_{16}[A] \\ -k(\alpha_{55} + \alpha_{66})[A] & 0.5k\alpha_{16}[B] & k\alpha_{16}[A] & k(\alpha_{55} + \alpha_{66})I - \beta_{11}[B] \end{bmatrix} \\
 [C_t] &= \begin{bmatrix} [0] & -2\gamma I & [0] & [0] \\ 2\gamma I & [0] & [0] & [0] \\ [0] & [0] & [0] & 2\mu_d \gamma I \\ [0] & [0] & -2\mu_d \gamma I & [0] \end{bmatrix} \quad [M_t] = \begin{bmatrix} I & [0] & [0] & [0] \\ [0] & I & [0] & [0] \\ [0] & [0] & \mu_d I & [0] \\ [0] & [0] & [0] & \mu_d I \end{bmatrix} \quad \{q\} = \begin{Bmatrix} \{v_0\} \\ \{w_0\} \\ \{\beta_y\} \\ \{\beta_z\} \end{Bmatrix}
 \end{aligned} \tag{25}$$

and boundary conditions can be modeled as:

$$[T_t]\{q\} = \{0\} \tag{26}$$

where matrix  $[T_t]$  is presented in Appendix B for various boundary conditions.

Let us divide grid points of solution into two groups; first and final points as boundary points ( $b$ ) and others as domain ones ( $d$ ). The equations of motion should be written only for the domain points [12]; thus Eqs. (21) and (24) should be rewritten as:

$$[\bar{K}_t]\{p\} = \lambda^2 [\bar{M}_t]\{p\} \tag{27a}$$

$$([\bar{K}_t] + \lambda[\bar{C}_t] + \lambda^2[\bar{M}_t])\{q\} = \{0\} \tag{27b}$$

In which, bar signs show the corresponded truncated non-square matrices. Eqs. (27a) and (27b) may be partitioned in order to separate the boundary and domain components as [12]:

$$[\bar{K}_t]_d \{p\}_d + [\bar{K}_t]_b \{p\}_b = \lambda^2 ([\bar{M}_t]_d \{p\}_d + [\bar{M}_t]_b \{p\}_b) \tag{28a}$$

$$[\bar{K}_t]_b \{q\}_b + [\bar{K}_t]_d \{q\}_d + \lambda([\bar{C}_t]_b \{q\}_b + [\bar{C}_t]_d \{q\}_d) + \lambda^2([\bar{M}_t]_b \{q\}_b + [\bar{M}_t]_d \{q\}_d) = \{0\} \tag{28b}$$

and in a similar manner, Eqs. (23) and (26) can be written as:

$$[T_t]_b \{p\}_b + [T_t]_d \{p\}_d = \{0\} \tag{29a}$$

$$[T_t]_b \{q\}_b + [T_t]_d \{q\}_d = \{0\} \tag{29b}$$

Using Eqs. (28) and (29), following eigen values equations can be derived:

$$[k_t]\{p\}_d = \lambda^2 [m_t]\{p\}_d \tag{30a}$$

$$[k_t]\{q\}_d + \lambda[c_t]\{q\}_d + \lambda^2 [m_t]\{q\}_d = \{0\} \tag{30b}$$

In which

$$[k_t] = [\bar{K}_t]_d - [\bar{K}_t]_b [T_t]_b^{-1} [T_t]_d \quad [m_t] = [\bar{M}_t]_d - [\bar{M}_t]_b [T_t]_b^{-1} [T_t]_d \tag{31}$$

$$[k_t] = [\bar{K}_t]_d - [\bar{K}_t]_b [T_t]_b^{-1} [T_t]_d \quad [c_t] = [\bar{C}_t]_d - [\bar{C}_t]_b [T_t]_b^{-1} [T_t]_d \quad [m_t] = [\bar{M}_t]_d - [\bar{M}_t]_b [T_t]_b^{-1} [T_t]_d$$

Unlike Eq. (30a), Eq. (30b) is not a standard eigen value equation and can be converted to a standard one as:

$$\begin{bmatrix} [0] & I \\ [k_t] & [c_t] \end{bmatrix} \begin{Bmatrix} \{q\}_d \\ \lambda \{q\}_d \end{Bmatrix} = \lambda \begin{bmatrix} I & [0] \\ [0] & -[m_t] \end{bmatrix} \begin{Bmatrix} \{q\}_d \\ \lambda \{q\}_d \end{Bmatrix} \quad (32)$$

## 5 EXACT SOLUTION

In order to be able to validate the proposed numerical solution, an exact solution for a specific case is presented. For a rotor with immovable supports, an exact solution can be found for longitudinal-torsional vibration. According to Eq. (16b), for longitudinal-torsional vibration following spatial functions can be considered for a rotor with immovable supports:

$$u_0(\zeta) = A_m \sin(m\pi\zeta) \quad \phi(\zeta) = B_n \sin(n\pi\zeta) \quad (33)$$

Substituting Eq. (33) into the Eq. (16a), following relation can be found for  $\lambda_{mn}$ :

$$\begin{vmatrix} m^2\pi^2 + \lambda_{mn}^2 & n^2\pi^2 k \alpha_{16} \\ m^2\pi^2 k \alpha_{16} & k \beta_{66} n^2 \pi^2 + 2\mu_d (\lambda_{mn}^2 - \gamma^2) \end{vmatrix} = 0 \quad (34)$$

## 6 NUMERICAL RESULTS AND DISCUSSION

In all of the numerical examples, a rotor made of Boron-Epoxy with the following properties is considered [13]:

$$\begin{aligned} E_1 = 146.85 \text{Gpa} \quad E_2 = E_3 = 11.03 \text{Gpa} \quad G_{12} = G_{13} = 6.21 \text{Gpa} \quad G_{23} = 3.86 \text{Gpa} \\ \nu_{12} = \nu_{13} = 0.28 \quad \nu_{23} = 0.5 \quad \rho = 1578 \text{Kg/m}^3 \end{aligned}$$

**Table 1**

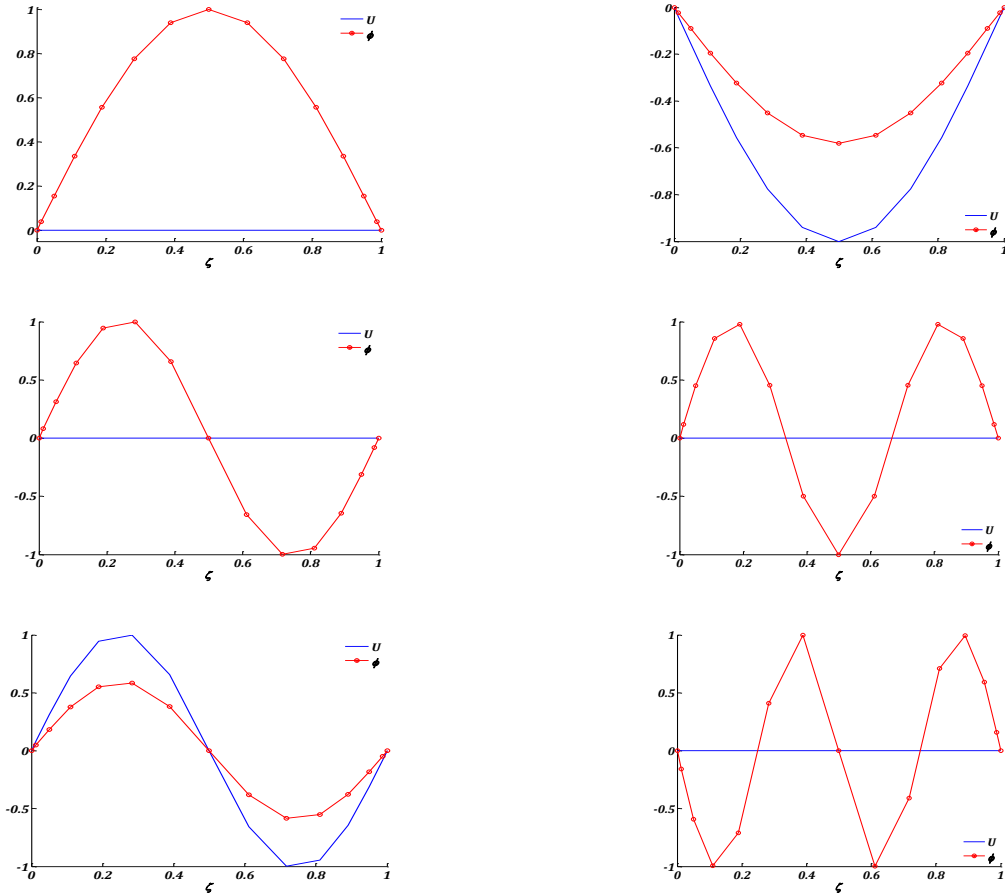
First six longitudinal-torsional and transverse frequencies of a clamped-clamped rotor.

Longitudinal-torsional						
DQM	1.927018	3.141813	3.86278	5.796597	6.283627	7.729931
Exact	1.927377	3.141813	3.863499	5.797675	6.283627	7.731365
	(m=0,n=1)	(m=1,n=1)	(m=0,n=2)	(m=0,n=3)	(m=2,n=2)	(m=0,n=4)
Transverse (Forward modes)						
DQM	0.541546	1.181134	2.065827	3.133866	4.337743	5.645814
Transverse (Backward modes)						
DQM	0.243661	0.888069	1.778292	2.851663	4.060101	5.371739

Also dimension of the rotor are considered as [9]:

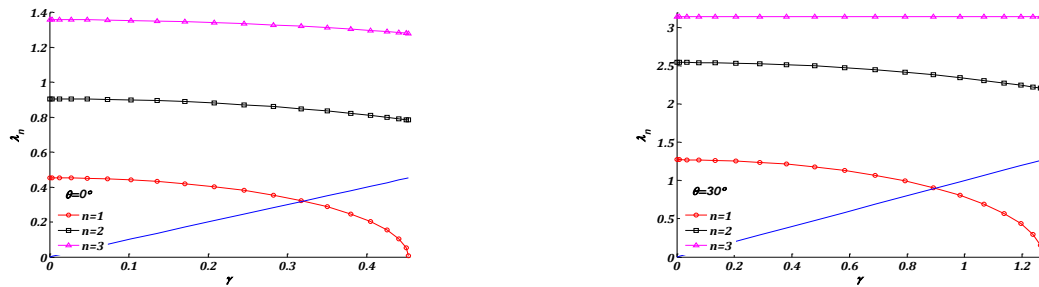
$$h_{ply} = 0.1321 \text{mm} \quad D_0 = 12.69 \text{cm} \quad L = 2.47 \text{m}$$

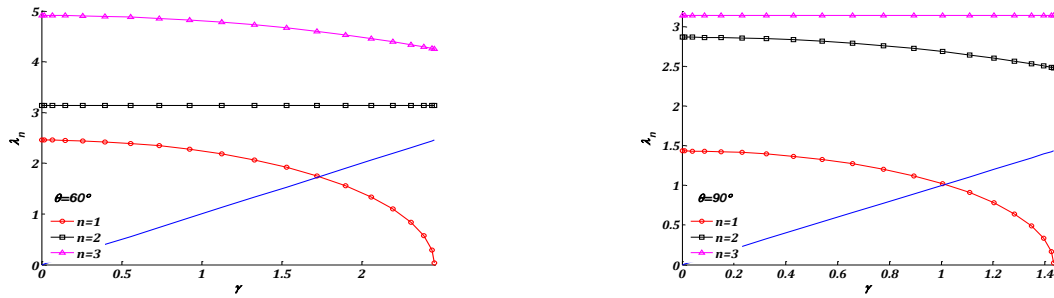
and shear correction factor is considered as  $k_s = 0.503$  [9]. Consider a rotor made of 10 layers with lamination angle  $\theta = 45^\circ$ . Table 1. shows the values of the first six longitudinal-torsional and transverse frequencies of a clamped-clamped rotor rotating with the angular velocity  $\gamma = 0.15$ . Number of grid points is considered as  $N = 15$ . Also, exact results obtained by Eq. (34) are presented in this table. As shown, results with high accuracy can be obtained; this table also confirms an evident conclusion that transverse frequencies are smaller than longitudinal-torsional ones. It indicates that rotor is more flexible in transverse deflection in comparison with longitudinal and torsional displacements. Also corresponding longitudinal-torsional modes are depicted in Fig. 2. There is an agreement between the modes obtained by DQM and corresponding values of m and n presented in Table 1., which confirms the accuracy and versatility of the proposed solution.



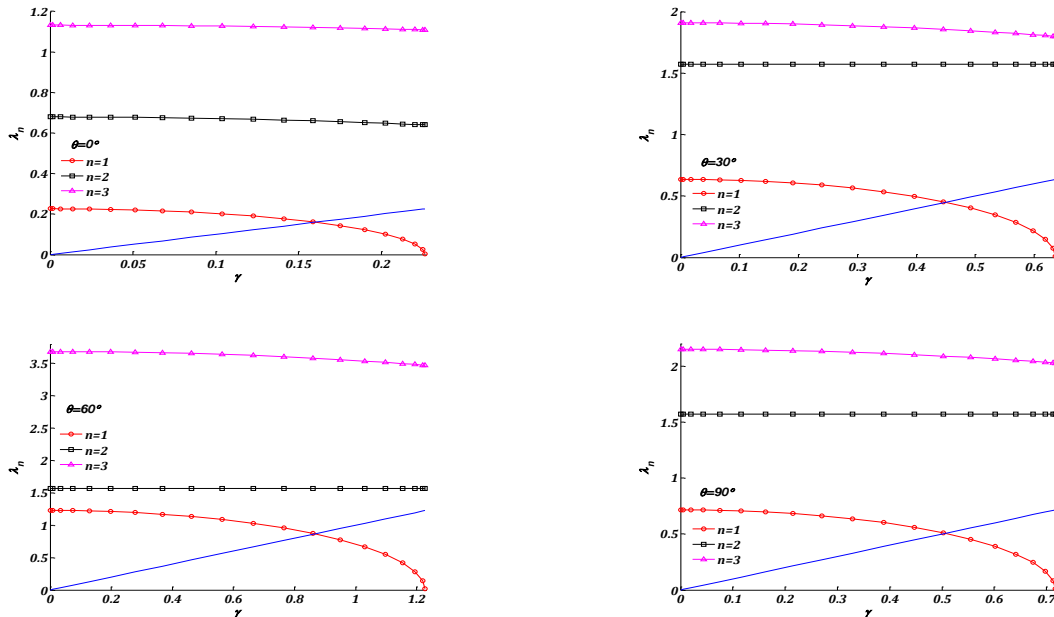
**Fig.2**  
Corresponding longitudinal-torsional modes.

In what follows, a rotor made of 10 layers as  $[\theta / -\theta]_5$  is considered. Fig. 3 shows variation of the first three longitudinal-torsional frequencies of a clamped-clamped rotor versus rotating speed (Campbell diagram) for various values of the lamination angle and similar diagrams are depicted for clamped-free one in Fig. 4. As depicted in these figures, all frequencies decrease as value of the rotating speed increases. For both longitudinal-torsional vibration and two plane transverse one, two kind of critical speeds are considered for the rotor; the resonance speed ( $\gamma_{cr}$ ), which happens as rotor rotates near one of the natural frequencies, and the instability speed ( $\gamma_{in}$ ), which occurs as value of the first natural frequency decreases to zero and rotor becomes unstable. Both resonance rotating speed and instability one are detectable in these figures.



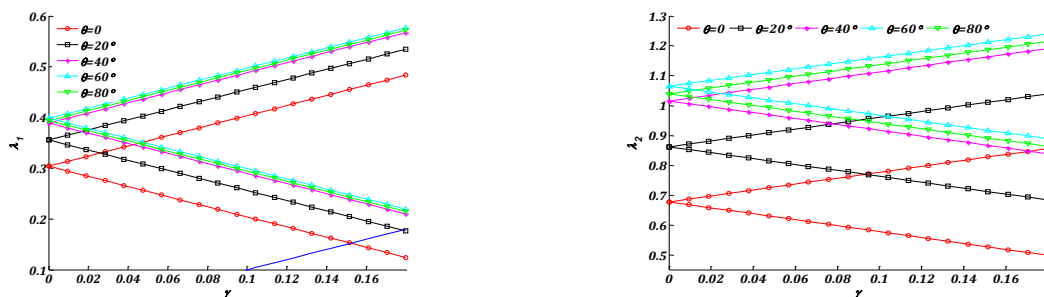


**Fig.3**  
Campbell diagram for the first three longitudinal-torsional frequencies of clamped-clamped rotor.



**Fig.4**  
Campbell diagram for the first three longitudinal-torsional frequencies of clamped-free rotor.

Figs. 5-8 show the variation of the first four backward and forward transverse frequencies of a clamped-clamped, clamped-simple, simple-simple and clamped-free rotors, versus rotating speed for various values of the lamination angle. As shown in these figures, for a non-rotating rotor, the value of the forward frequencies (ascending lines) and backward ones (descending lines) are the same; but because of gyroscopic effects, as the value of the velocity of spin increases, forward frequencies increase and backward ones decrease. These figures also show the line of synchronous whirling; intersection of this line with the Campbell diagram determines the critical speeds, which should be avoided.



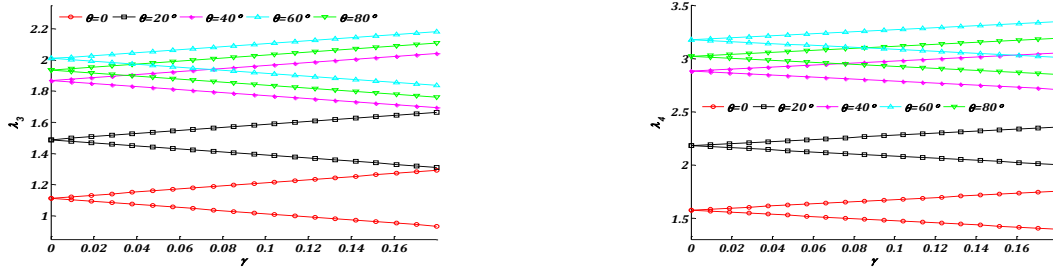


**Fig.5**  
Campbell diagram for the first four transverse frequencies of clamped-clamped rotor.

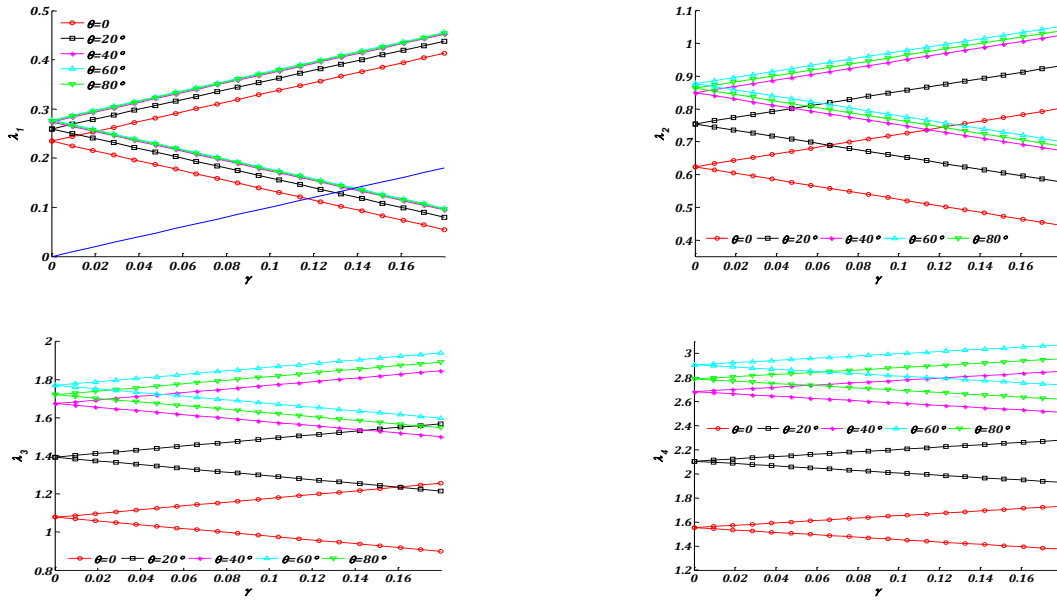


**Fig.6**  
Campbell diagram for the first four transverse frequencies of clamped-simple rotor.

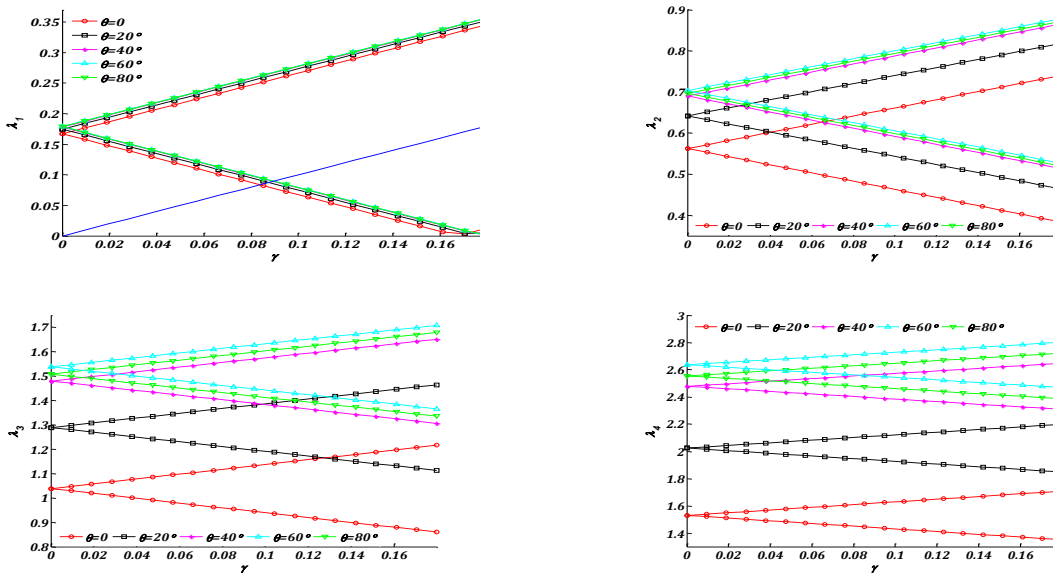


**Fig.7**  
Campbell diagram for the first four transverse frequencies of simple-simple rotor.

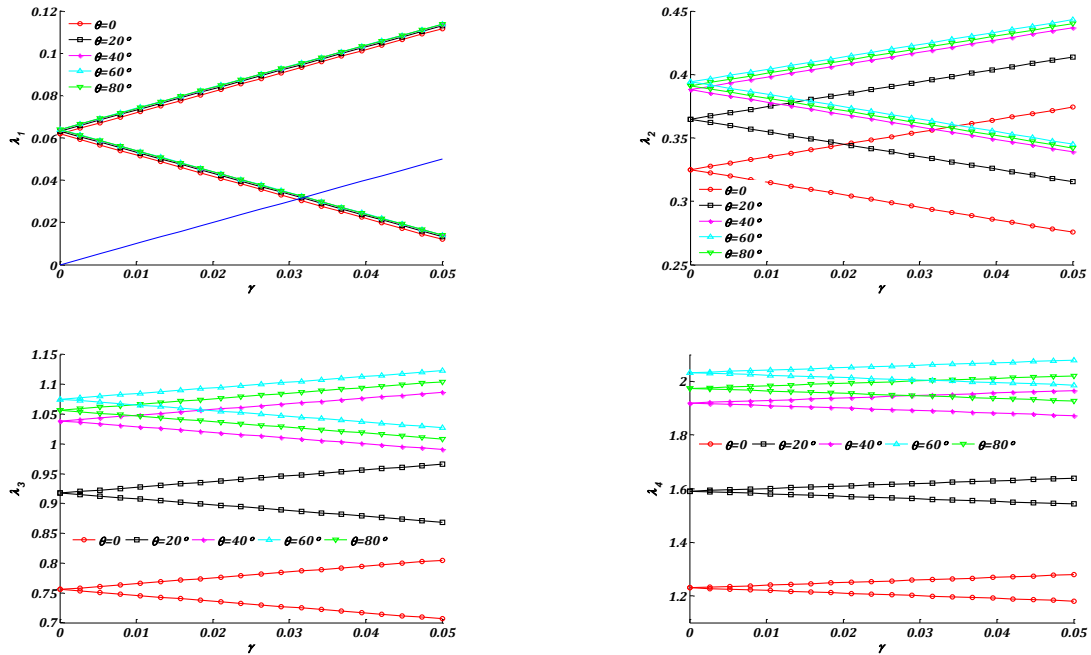


**Fig.8**  
Campbell diagram for the first four transverse frequencies of clamped-free rotor.

Also for  $\theta = 40^\circ$  and  $\gamma = 0.05$ , the corresponding first two forward and backward modes are depicted in Figs. 9 to 12 for clamped-clamped, clamped-simple, simple-simple and clamped-free rotors, respectively.

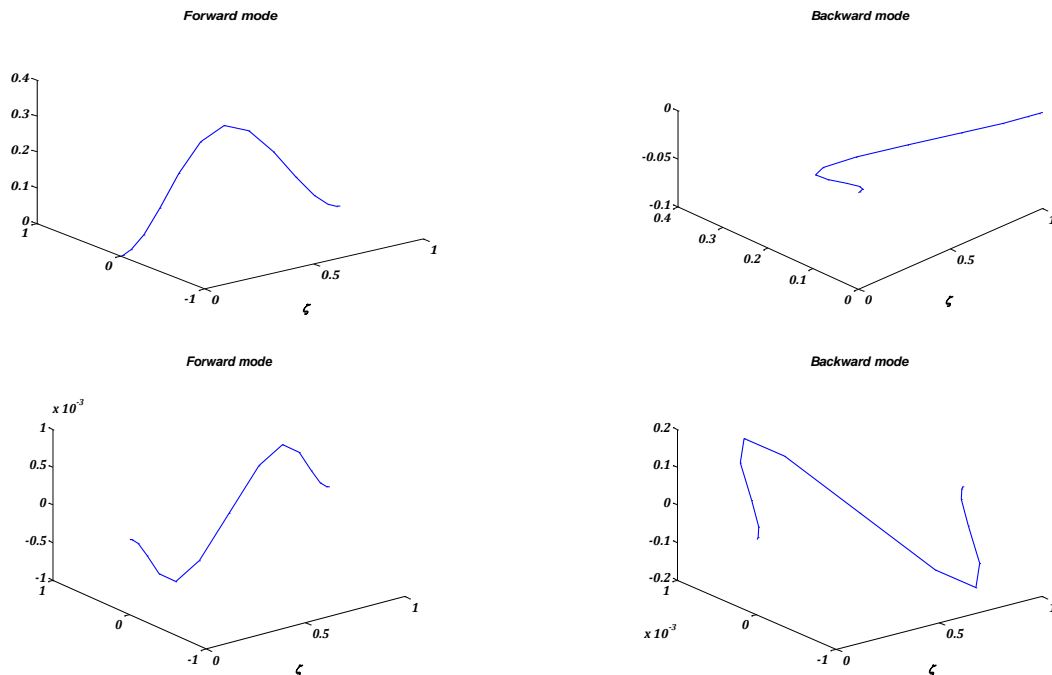


**Fig.9**  
Corresponding modes for the first two transverse modes of clamped-clamped rotor with  $\theta = 45^\circ$  and  $\gamma = 0.05$ .

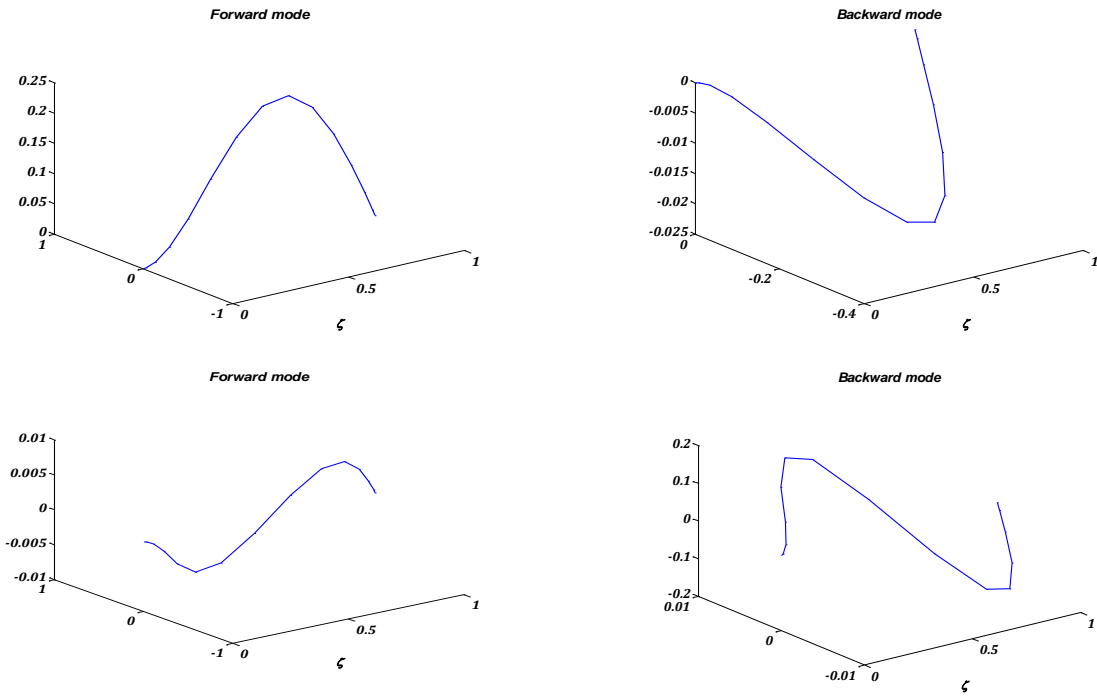


**Fig.10**  
Corresponding modes for the first two transverse modes of clamped-simple rotor with  $\theta = 45$  and  $\gamma = 0.05$ .

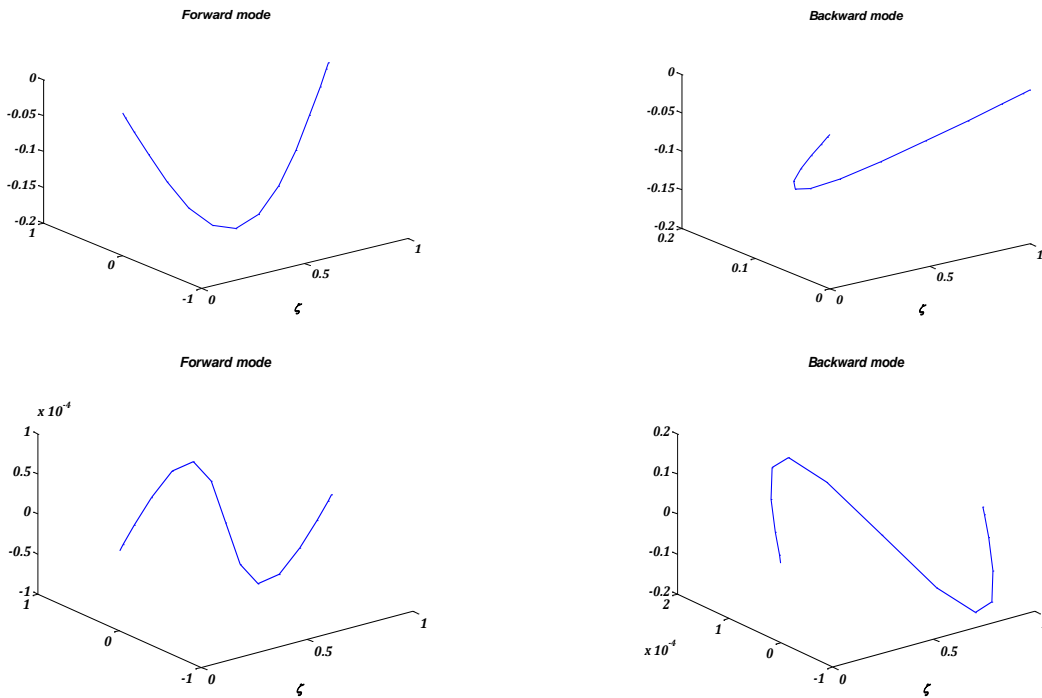


**Fig.11**  
Corresponding modes for the first two transverse modes of simple-simple rotor with  $\theta = 45$  and  $\gamma = 0.05$ .

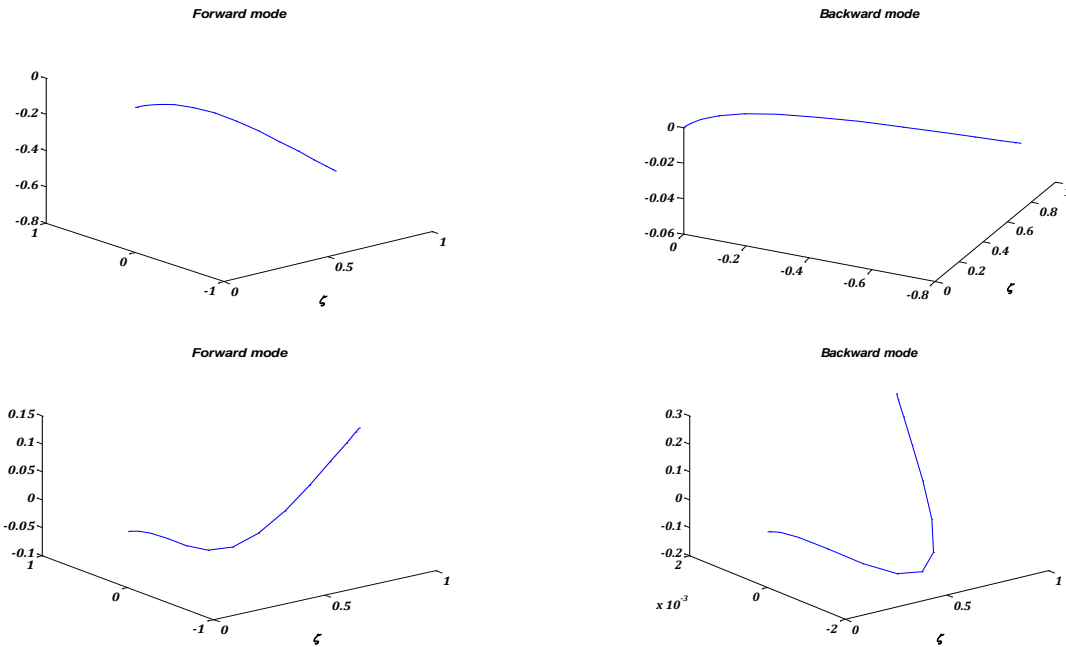


Fig.12

Corresponding modes for the first two transverse modes of clamped-free rotor with  $\theta = 45$  and  $\gamma = 0.05$ .

Figs. 13 and 14 show the variation of the longitudinal-torsional and transverse critical speeds versus lamination angle. As these figures show, for both kind of vibrations, both resonance and instability speeds increase as the value of the lamination angle grows from 0 to near  $60^\circ$  and then decrease as value of the lamination angle grows from near  $60^\circ$  to  $90^\circ$ . It should be noted that in order to be able to see variation of the critical frequencies for all boundary conditions, all of them are divided to the corresponding values of  $\theta = 0$ ; in other words  $\Gamma_{cr} = \gamma_{cr} / \gamma_{cr}(\theta = 0)$  and  $\Gamma_{in} = \gamma_{in} / \gamma_{in}(\theta = 0)$ .

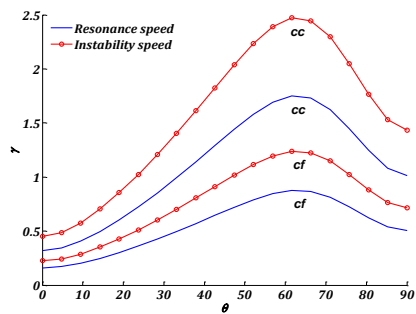


Fig.13

Variation of the longitudinal-torsional critical speeds versus lamination angle.

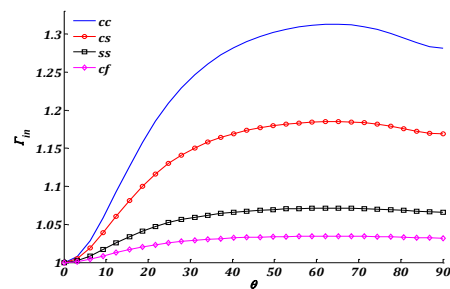
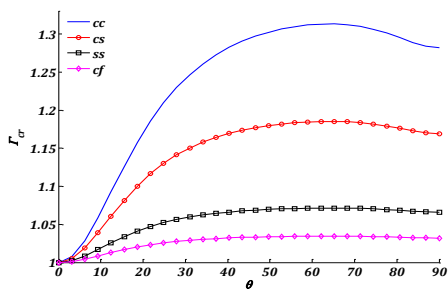


Fig.14

Variation of the transverse critical speeds versus lamination angle.

**7 CONCLUSIONS**

Using Hamilton principle, the set of governing equations and boundary conditions of longitudinal-torsional and two plane transverse vibration analyses of a composite Timoshenko rotor were derived and solved numerically by DQM. Comparison between obtained numerical results and exact solution which was proposed for a special case, confirmed the accuracy of the proposed solution. Numerical results showed that for longitudinal-torsional vibration, all frequencies decrease as the value of the rotating speed increases. Moreover, for transverse one, for a non-rotating rotor, the value of the forward and backward frequencies are the same. Owing to gyroscopic effects, however, as the value of the velocity of spin increases, forward frequencies increase and backward frequencies decrease. Numerical results showed that for both longitudinal-torsional and transverse vibration, all natural frequencies and therefore both resonance and instability critical rotating speeds increase as value of the lamination angle grows from 0 to near 60° and then decrease as value of the lamination angle grows from near 60° to 90° .

**APPENDIX A**

As said in Eq. (10),  $C'_{ijn}$  are the effective elastic constants of the  $n^{th}$  layer which connect components of stress and strain as:

$$\begin{pmatrix} \sigma_{xx} \\ \sigma_{\theta\theta} \\ \sigma_{rr} \\ \tau_{r\theta} \\ \tau_{xr} \\ \tau_{x\theta} \end{pmatrix} = \begin{bmatrix} C'_{11} & C'_{12} & C'_{13} & 0 & 0 & C'_{16} \\ C'_{12} & C'_{22} & C'_{23} & 0 & 0 & C'_{26} \\ C'_{13} & C'_{23} & C'_{33} & 0 & 0 & C'_{36} \\ 0 & 0 & 0 & C'_{44} & C'_{45} & 0 \\ 0 & 0 & 0 & C'_{45} & C'_{55} & 0 \\ C'_{16} & C'_{26} & C'_{36} & 0 & 0 & C'_{66} \end{bmatrix} \begin{pmatrix} \epsilon_{xx} \\ \epsilon_{\theta\theta} \\ \epsilon_{rr} \\ \gamma_{r\theta} \\ \gamma_{xr} \\ \gamma_{x\theta} \end{pmatrix} \tag{A.1}$$

These constants are related to the elastic constants of principal axes ( $C_{ij}$ ) and lamination angle  $\theta$  as [14]:

$$\begin{aligned} C'_{11} &= C_{11} \cos^4 \theta + 2(C_{12} + 2C_{66}) \sin^2 \theta \cos^2 \theta + C_{22} \sin^4 \theta \\ C'_{16} &= (C_{11} - C_{12} - 2C_{66}) \sin \theta \cos^3 \theta + (2C_{66} + C_{12} - C_{22}) \sin^3 \theta \cos \theta \\ C'_{55} &= C_{55} \cos^2 \theta + C_{44} \sin^2 \theta \\ C'_{66} &= (C_{11} + C_{22} - 2C_{12} - 2C_{66}) \sin^2 \theta \cos^2 \theta + C_{66} (\sin^4 \theta + \cos^4 \theta) \end{aligned} \tag{A.2}$$

Also elastic constants of principal axes can be calculated using following relations [14]:

$$\begin{aligned} C_{11} &= \frac{1 - \nu_{23}^2}{E_2 E_3 \Delta} & C_{12} &= \frac{\nu_{12} + \nu_{32} \nu_{13}}{E_1 E_3 \Delta} & C_{22} &= \frac{1 - \nu_{13} \nu_{31}}{E_1 E_3 \Delta} & C_{44} &= G_{23} & C_{55} &= G_{13} & C_{66} &= G_{12} \\ \Delta &= \frac{1 - \nu_{12} \nu_{21} - \nu_{23} \nu_{32} - \nu_{31} \nu_{13} - 2\nu_{21} \nu_{32} \nu_{13}}{E_1 E_2 E_3} \end{aligned} \tag{A.3}$$

**APPENDIX B**

For longitudinal-torsional vibration, the matrix of boundary conditions appeared in Eq. (23) can be defined for clamped (C), simple (S) or free (F) conditions as:

$$\begin{aligned}
 & \text{CC, CS or SS} & & \text{CF} \\
 [T_{tt}] = & \begin{cases} \delta_{1j} & i = 1, j = 1, \dots, N \\ \delta_{1(j-N)} & i = 2, j = N + 1, \dots, 2N \\ \delta_{Nj} & i = 3, j = 1, \dots, N \\ \delta_{N(j-N)} & i = 4, j = N + 1, \dots, 2N \\ 0 & \text{else} \end{cases} & [T_{tt}] = & \begin{cases} \delta_{1j} & i = 1, j = 1, \dots, N \\ \delta_{1(j-N)} & i = 2, j = N + 1, \dots, 2N \\ A_{Nj} & i = 3, j = 1, \dots, N \\ k \alpha_{16} A_{N(j-N)} & i = 3, j = N + 1, \dots, 2N \\ \alpha_{16} A_{Nj} & i = 4, j = 1, \dots, N \\ \beta_{66} A_{N(j-N)} & i = 4, j = N + 1, \dots, 2N \\ 0 & \text{else} \end{cases}
 \end{aligned} \tag{B.1}$$

and for transverse vibration, the matrix of boundary conditions appeared in Eq. (26) can be defined as:

$$\begin{aligned}
 & \text{CC} & & \text{CS} \\
 [T_t] = & \begin{cases} \delta_{1j} & i = 1, j = 1, \dots, N \\ \delta_{1(j-N)} & i = 2, j = N + 1, \dots, 2N \\ \delta_{1(j-2N)} & i = 3, j = 2N + 1, \dots, 3N \\ \delta_{1(j-3N)} & i = 4, j = 3N + 1, \dots, 4N \\ \delta_{Nj} & i = 5, j = 1, \dots, N \\ \delta_{N(j-N)} & i = 6, j = N + 1, \dots, 2N \\ \delta_{N(j-2N)} & i = 7, j = 2N + 1, \dots, 3N \\ \delta_{N(j-3N)} & i = 8, j = 3N + 1, \dots, 4N \\ 0 & \text{else} \end{cases} & [T_t] = & \begin{cases} \delta_{1j} & i = 1, j = 1, \dots, N \\ \delta_{1(j-N)} & i = 2, j = N + 1, \dots, 2N \\ \delta_{1(j-2N)} & i = 3, j = 2N + 1, \dots, 3N \\ \delta_{1(j-3N)} & i = 4, j = 3N + 1, \dots, 4N \\ \delta_{Nj} & i = 5, j = 1, \dots, N \\ \delta_{N(j-N)} & i = 6, j = N + 1, \dots, 2N \\ -0.5k \alpha_{16} A_{Nj} & i = 7, j = 1, \dots, N \\ \beta_{11} A_{N(j-2N)} & i = 7, j = 2N + 1, \dots, 3N \\ 0.5k \alpha_{16} \delta_{N(j-3N)} & i = 7, j = 3N + 1, \dots, 4N \\ -0.5k \alpha_{16} A_{N(j-N)} & i = 8, j = N + 1, \dots, 2N \\ -0.5k \alpha_{16} \delta_{N(j-2N)} & i = 8, j = 2N + 1, \dots, 3N \\ \beta_{11} A_{N(j-3N)} & i = 8, j = 3N + 1, \dots, 4N \\ 0 & \text{else} \end{cases} \\
 & \text{SS} & & \text{CF} \\
 [T_t] = & \begin{cases} \delta_{1j} & i = 1, j = 1, \dots, N \\ \delta_{1(j-N)} & i = 1, j = N + 1, \dots, 2N \\ -0.5k \alpha_{16} A_{1j} & i = 2, j = 1, \dots, N \\ \beta_{11} A_{1(j-2N)} & i = 2, j = 2N + 1, \dots, 3N \\ 0.5k \alpha_{16} \delta_{1(j-3N)} & i = 3, j = 3N + 1, \dots, 4N \\ -0.5k \alpha_{16} A_{1(j-N)} & i = 3, j = N + 1, \dots, 2N \\ -0.5k \alpha_{16} \delta_{1(j-2N)} & i = 4, j = 2N + 1, \dots, 3N \\ \beta_{11} A_{1(j-3N)} & i = 4, j = 3N + 1, \dots, 4N \\ \delta_{Nj} & i = 5, j = 1, \dots, N \\ \delta_{N(j-N)} & i = 6, j = N + 1, \dots, 2N \\ -0.5k \alpha_{16} A_{Nj} & i = 7, j = 1, \dots, N \\ \beta_{11} A_{N(j-2N)} & i = 7, j = 2N + 1, \dots, 3N \\ 0.5k \alpha_{16} \delta_{N(j-3N)} & i = 7, j = 3N + 1, \dots, 4N \\ -0.5k \alpha_{16} A_{N(j-N)} & i = 8, j = N + 1, \dots, 2N \\ -0.5k \alpha_{16} \delta_{N(j-2N)} & i = 8, j = 2N + 1, \dots, 3N \\ \beta_{11} A_{N(j-3N)} & i = 8, j = 3N + 1, \dots, 4N \\ 0 & \text{else} \end{cases} & [T_t] = & \begin{cases} \delta_{1j} & i = 1, j = 1, \dots, N \\ \delta_{1(j-N)} & i = 2, j = N + 1, \dots, 2N \\ \delta_{1(j-2N)} & i = 3, j = 2N + 1, \dots, 3N \\ \delta_{1(j-3N)} & i = 4, j = 3N + 1, \dots, 4N \\ -(\alpha_{55} + \alpha_{66}) A_{Nj} & i = 5, j = 1, \dots, N \\ 0.5 \alpha_{16} A_{N(j-2N)} & i = 5, j = 2N + 1, \dots, 3N \\ (\alpha_{55} + \alpha_{66}) \delta_{N(j-3N)} & i = 5, j = 3N + 1, \dots, 4N \\ -(\alpha_{55} + \alpha_{66}) A_{Nj} & i = 6, j = N + 1, \dots, 2N \\ -(\alpha_{55} + \alpha_{66}) \delta_{N(j-2N)} & i = 6, j = 2N + 1, \dots, 3N \\ 0.5 \alpha_{16} A_{N(j-3N)} & i = 6, j = 3N + 1, \dots, 4N \\ -0.5k \alpha_{16} A_{Nj} & i = 7, j = 1, \dots, N \\ \beta_{11} A_{N(j-2N)} & i = 7, j = 2N + 1, \dots, 3N \\ 0.5k \alpha_{16} \delta_{N(j-3N)} & i = 7, j = 3N + 1, \dots, 4N \\ -0.5k \alpha_{16} A_{N(j-N)} & i = 8, j = N + 1, \dots, 2N \\ -0.5k \alpha_{16} \delta_{N(j-2N)} & i = 8, j = 2N + 1, \dots, 3N \\ \beta_{11} A_{N(j-3N)} & i = 8, j = 3N + 1, \dots, 4N \\ 0 & \text{else} \end{cases}
 \end{aligned} \tag{B.2}$$

## REFERENCES

- [1] Zu J., Hans R.P., 1992, Natural frequencies and normal modes of a spinning beam with general boundary conditions, *Journal of Applied Mechanics, Transactions ASME* **59**:197-204.
- [2] Zu J., Melanson J., 1998, Natural frequencies and normal modes of for externally damped spinning Timoshenko beams with general boundary conditions, *Journal of Applied Mechanics, Transactions ASME* **65**:770-772.
- [3] Dos Reis H. L. M., Goldman R. B., Verstrate P. H., 1987, Thin-walled laminated composite cylindrical tubes—part III: critical speed analysis, *Journal of Composites Technology and Research* **9**(2):58-62.
- [4] Gupta K., Singh S. E., 1996, Dynamics of composite rotors, *Proceedings of the Indo-US Symposium on Emerging Trends in Vibration and Noise Engineering*, New Delhi, India.
- [5] Bert C.W., 1992, The effects of bending twisting coupling on the critical speed of drive shafts, *Composite Materials, 6th Japan/US Conference*, Orlando Lancaster.
- [6] Kim C.D., Bert C.W., 1993, Critical speed analysis of laminated composite, hollow drive shafts, *Composites Engineering* **3**:633-643.
- [7] Banerjee J.R., Su H., 2006, Dynamic stiffness formulation and free vibration analysis of a spinning composite beam, *Computers and Structures* **84**: 1208-1214.
- [8] Chang M.Y., Chen J.K., Chang C.Y., 2004, A simple spinning laminated composite shaft model, *International Journal of Solids and Structures* **41**(4): 637-662.
- [9] Boukhalfa A., Hadjoui A., 2010, Free vibration analysis of an embarked rotating composite shaft using the hp-version of the FEM, *Latin American Journal of Solids and Structures* **7**: 105-141.
- [10] Choi S.H., Pierre C., Ulsoy A.G., 1992, Consistent modeling of rotating Timoshenko shafts subject to axial loads, *Journal of Vibration and Acoustics* **114**: 249-259.
- [11] Bert C.W., Malik M., 1996, Differential quadrature method in computational mechanics: A review, *Applied Mechanics Reviews* **49**: 1-28.
- [12] Du H, Lim M.K., Lin N.R., 1994, Application of generalized differential quadrature method to structural problems, *International Journal for Numerical Methods in Engineering* **37**:1881-1896.
- [13] Sun J., Ruzicka M., 2006, A calculation method of hollow circular composite beam under general loadings, *Bulletin of Applied Mechanics* **3**(12): 105-114.
- [14] Reddy J.N., 2004, *Mechanics of Laminated Composite Plates and Shells: Theory and Analysis*, CRC Press, Boca Raton, FL.